doi: 10.1109/EUROSOI-ULIS49407.2020.9365285 - ©2021 IEEE. Personal use is permitted, but republication/redistribution requires IEEE permission.
See http://www.ieee.org/publications standards/publications/rights/index.html for more information.

Modeling Selectivity and Cross-sensitivity in membrane-based potentiometric sensors

Leandro Julian Mele*‡, Pierpaolo Palestri* and Luca Selmi†
*DPIA, University of Udine, 33100, Udine, Italy.
†DIEF, University of Modena and Reggio Emilia, 44100, Modena, Italy.
‡Corresponding author. Email: mele.leandrojulian@spes.uniud.it

***Abstract*—We propose a steady state model for ion selective membranes (ISM) as selectivity element in potentiometric sensors. The model solves the Poisson-Boltzmann equation, coupled to distributed chemical reactions between ionophores and two types of competing ions. We show that a Donnan potential arises when ionic sites are present, while selectivity is achieved only if using ionophore-doped ISMs. The model allows to evaluate cross-sensitivities and can explain steady state non-Nernstian responses. We also provide an application example of sensor parameter design supported by the proposed model.**

***Keywords*—ion-selective-membranes; device simulation; potentiometric sensors.**

I. Introduction

The combination of integrated silicon FETs with ion selective membranes (ISMs) has greatly extended the application domains of potentiometric sensors [1], [2]. Such device consists of replacing the gate of a FET with an ISM in contact with the electrolyte chamber containing the target analytes (Fig. 1.a). If the bulk electrolyte is kept at a fixed potential V_{fg} (by the fluid gate reference electrode), a voltage drop at the membrane/electrolyte interface arises (the Donnan potential [3]), that shifts the threshold voltage of the underlying FET. ISMs operate over a wide range of ion concentrations and ion species thus enabling excellent selectivity [4].

In this work, we propose a new model to describe the electrolyte/membrane interaction that goes beyond the widely employed boundary potential approach [5], as it handles spatially distributed chemical reactions and complex structures. The ultimate goal is to support improvements of the sensor design to enhance selectivity and reduce cross-sensitivities.

II. Device model

The response of ISMs arises at the membrane/electrolyte interface due to the permeability of ions and their local interactions with ionic sites (see below). The electrostatic potential, ψ, is given by the non-linear Poisson-Boltzmann (PB) equation that includes fixed (ρ_f), and mobile (ρ_m) charges, and in 1D reads:

$$\frac{d}{dx}\left(\varepsilon(x)\frac{d\psi(x)}{dx}\right) = -\left(\rho_m(x) + \rho_f(x)\right) \qquad (1)$$

We acknowledge funding from the European Unions Horizon 2020 research and innovation programme under grant agreement No 862882 (IN-FET project) via the IUNET Consortium.

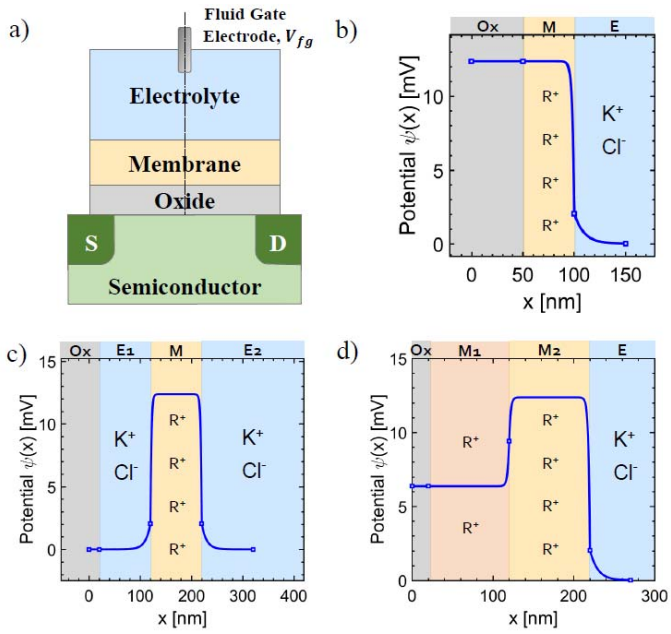

Fig. 1. Calculated electrostatic potential across the device layers for the three case studies defined in [3]. 'Ox' denotes the metal oxide of the underlying FET device, 'E_i' the electrolyte and 'M_i' the membrane layer(s), respectively. Case b) refers to the dashed cut line in a). Case c) refers to a structure similar to plot a) but with an electrolyte E_1 between the oxide and the ISM, while in case d) we have a stack with two different membranes M_1 and M_2. The membrane layers contain ionic sites, namely, fixed charges depicted with R^+ (in this case positively charged) while the electrolytes contain the mobile ionic species (e.g. K^+ and Cl^-).

Electrochemical equilibrium of those ions that cross the membrane interface generates a potential drop $\Delta\psi$ within a few nm distance. This drop is the integral of the electric field that forces ion drift to equilibrate the diffusion, eventually giving zero net current. The resulting mobile charge distribution is then given by the sum of Boltzmann distributions,

$$\rho_m = q\sum_{i=1}^{N_{sp}} z_i a_i^{\infty}\left\{\begin{matrix}1\\k_i\end{matrix}\right\}\exp\left(-\frac{z_i q}{k_B T}\psi(x)\right), \qquad (2)$$

where a_i^{∞} is the equilibrated bulk concentration of the ith ionic species in the electrolyte, N_{sp} the number of ionized species with their valence z_i and the coefficient k_i (that only applies in the membrane layer, while "1" is used in the electrolyte), hereafter simply denoted as 'affinity', is defined through the

doi: 10.1109/EUROSOI-ULIS49407.2020.9365285 - ©2021 IEEE. Personal use is permitted, but republication/redistribution requires IEEE permission.
See http://www.ieee.org/publications standards/publications/rights/index.html for more information.

standard chemical potentials μ_i^0 of the species in the two layers as [5]

$$k_i = \exp\left(\left[\mu_i^0(el) - \mu_i^0(mem)\right]/(k_B T)\right). \quad (3)$$

In fact, since $\Delta\psi$ is experienced by all species that can enter the membrane, the equilibrated bulk concentrations in the two regions are related by a constant factor.

III. Ionic sites (fixed charges)

ISMs naturally [6] or intentionally contain ionic sites (i.e. hydrophobic ions with very low mobility confined in the membrane phase) and denoted R^+ in Fig. 1. Here, they are modelled as uniformly distributed fixed charges, ρ_f, that oppose the extraction from the electrolyte of ions of the same charge sign and, owing to electroneutrality, tend to set the concentration of counter-ions in the membrane conferring Nernstian responses to the change of individual counterion species. Thus, the sole presence of ionic sites yields membrane response and consequently generates a FET threshold voltage shift, but no selectivity since only the charge sign of the counter-ion matters. Fig. 1 shows the simulated $\psi(x)$ for the three scenarios defined in [3]: the classical ISM with membrane deposited on a solid insulator (a,b); an electrolyte layer interposed between insulator and ISM (e.g. after membrane detachment with water infiltration, c) and a stack of two ISMs (e.g. organic functionalized devices), d). In all cases Donnan equilibrium (i.e. ionic and potential gradients produced by a semipermeable layer separating ionic solutions) is established [3]. Interestingly, in case c) the free ions in the layer E_1 screen out completely the membrane potential, thus giving no net voltage build-up at the sensor surface (Ox) and zero sensitivity. These demonstrate the importance of membrane adhesion to the oxide layer to achieve good sensitivity. In case d), the different concentration of ionic sites in M_1 and M_2 creates an additional potential difference between the two layers, so that only the net potential drop across the membrane shifts the FET threshold.

The concentration of ionic sites impacts the Nernstian range of the sensor response. Fig. 2.a shows the case of a KCl calibration curve, where the concentration of the ionic sites R^- (here negatively charged) is changed. As expected, the absence of ionic sites (Fig. 2.a, open circles) gives no membrane response as Cl^- ions are co-extracted together with target ions K^+. Low concentrations of ionic sites (i.e. 1 mM) are instead enough to produce Nernstian responses to K^+ ions, but for a range of concentrations smaller than those of the ionic sites. In fact, as the salt concentration in the electrolyte approaches the ionic sites' concentration, the latter can no longer prevent co-extraction of Cl^- ions. Hence, higher concentrations of ionic sites (diamonds in Fig. 2.a) provide Nernstian responses for a larger range of target ion concentrations.

The impact of k_i is shown in Fig. 2.b. In general, lower affinity values tend to enlarge the range of Nernstian response, since higher salt concentrations in the electrolyte are necessary to make the concentration of absorbed ions balance or exceed the one of the ionic sites. On the other hand, different k_i values of electrolyte species can turn into intrinsic selectivity. For example, in Fig. 2.b the range of Nernstian response to K^+ ions is higher when k_{Cl} is smaller. In fact, if a lower fraction of Cl^- ions can enter the membrane, then less interference is experienced by the target K^+ ions in the range at which ionic sites can still play their part.

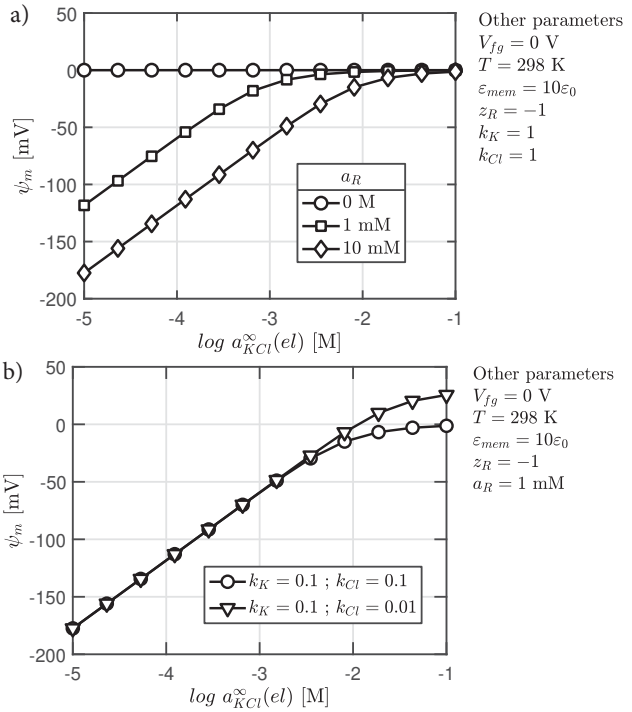

Fig. 2. Simulated membrane potential vs the concentration of KCl salt in the electrolyte. a) different concentrations of ionic sites and, b), the effect of the ions affinity constants are considered.

IV. Ionophores and selectivity

Ionic sites provide intrinsic selectivity only as long as the different lipophilicity of ions results in different affinity constants [7]. However, such selective feature is usually not controllable when designing the ISM material. On the contrary, ionophores (i.e., mobile lipophilic compounds confined in the membrane layer, designed to specifically bind the target ion) facilitate the transport of target ions in the membrane phase with respect to its interferents [8] and thus effectively increase the selectivity. To capture also this effect, we extended the total boundary potential model developed in [5] to an arbitrary sequence of layers of ISMs and electrolytes, and applied it to the stack of Fig. 1.a. Denoting with I the target ion and J the interferent ion, we define the following reactions with ionophores, L, inside the membrane:

$$\begin{aligned} I + n_I L \leftrightharpoons IL_{n_I} \quad &\Longrightarrow \quad \beta_{IL} = \frac{a_{IL}}{a_I a_L^{n_I}} \\ J + n_J L \leftrightharpoons JL_{n_J} \quad &\Longrightarrow \quad \beta_{JL} = \frac{a_{JL}}{a_J a_L^{n_J}} \end{aligned} \quad (4)$$

where β_{IL} and β_{JL} are association constants and n_I and n_J are the respective stoichiometric coefficients. Concentrations of free ions in Eq. 4 follow Boltzmann distributions (Eq. 2).

doi: 10.1109/EUROSOI-ULIS49407.2020.9365285 - ©2021 IEEE. Personal use is permitted, but republication/redistribution requires IEEE permission.

Conservation of the total number of ionophores L_{tot} (bonded and free) imposes

$$a_L = L_{tot} - n_I a_{IL} - n_J a_{JL}. \quad (5)$$

Insertion of Eq. 5 into Eq. 4 and use of Boltzmann statistics (Eq. 2) gives the expression of the local equilibrium concentration of the complexes a_{IL} and a_{JL}. These concentrations indirectly depend on those of the mobile species and can be considered as additional fixed charges of the total ρ_f. Explicit closed form expressions for a_{IL} and a_{JL} are crucial since they must be computed at each iteration of a self-consistent (e.g. Newton-Raphson) loop upon coupling of the Poisson and Boltzmann Eqs. 1 and 2. In this work we found analytical expressions of such concentrations for stoichiometric coefficients up to 3. The computation flowchart is depicted in Fig. 3.

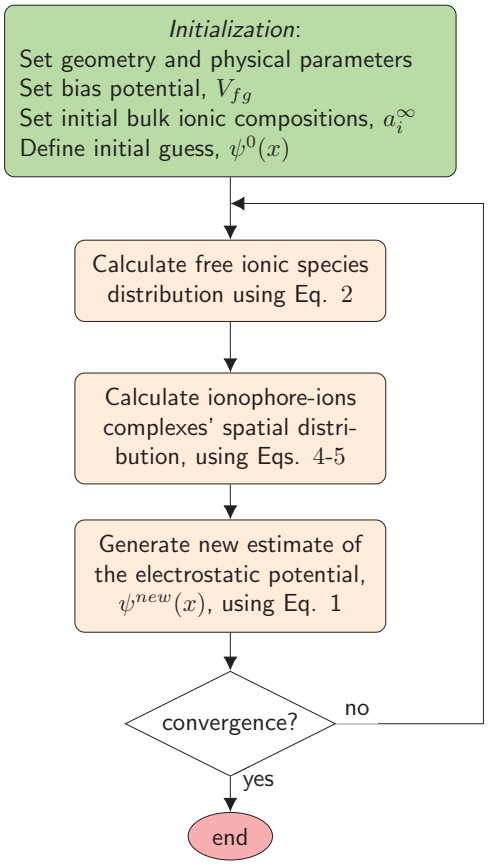

Fig. 3. Flowchart to solve the PB loop coupled to distributed chemical reactions in ISMs using iterative solutions. In this work we used analytically derived Jacobian expressions to avoid lengthy simulation times and convergence issues.

In this analysis, we only consider steady solutions (i.e. drift and diffusion processes are at equilibrium) and assume the electrolyte as an infinite reservoir of ions. Fig. 4 validates the model by comparing our simulations with the model in [5], where the interface potential is simply forced equal to the difference between the bulk potentials in the membrane and electrolyte. Simulations are designed to yield sub-, inverted- and super-Nernstian responses, respectively and the agreement with [5] is good over a large range of concentrations. Compared to [5], our model includes ionic screening and double layer formation at charged interfaces, owing to the coupled PB system of equations. Therefore, it provides a more realistic simulation framework and it is amenable for 2D and 3D implementation.

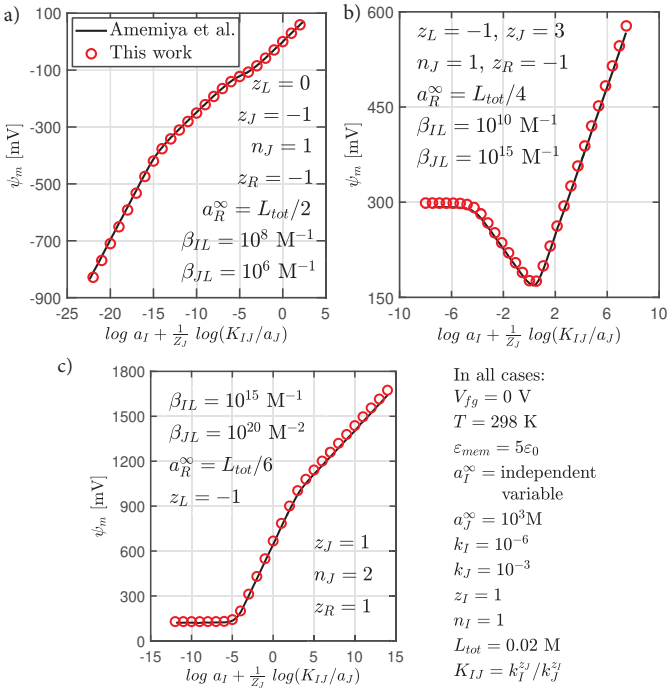

Fig. 4. Membrane potential calculated in [5] compared with our model for a) sub, b) inverted and c) super-Nernstian responses, respectively, and list of parameters used. The bulk concentrations refer to the electrolyte region.

The model also provides useful insights on the sensor response. For example, Fig. 5.a shows the effect of the ionophore-target ion complex strength on the potential shift, where K^+ is the target ion, Cl^- and Na^+ are background ions that do not interact with ligands. It can be seen that strong KL^+ complexes (i.e. high β_{KL} constants) can significantly lower the limits of detection (leftward shift of the curves) reducing the effect of the target co-ion Na^+ penetration. However, a too strong KL^+ complex decrease the upper limit of detection, that is, the highest concentration before the onset of an undesired inverted response and non-monotonicity. This is due to counter-ions (Cl^-) extraction from the electrolyte i.e. the so called Donnan failure [9]. Figs. 5.b-c report the electrostatic potential and ionic concentration profiles, respectively, in the region of Nernstian response (red mark in Fig. 5.a). The ionic concentration in the membrane is higher than in the electrolyte which reflects in a shorter Debye screening length and a faster potential decay (Fig. 5.b). The presence of ionophores and ionic sites determines the ionic concentration inside the membrane as apparent in Fig. 5.c, where all the free ionic species in the membrane layer (i.e. K^+, Na^+ and Cl^-) have negligible concentrations. The mechanism of fixing the concentration of the target ion in the membrane is essential to obtain Nernstian responses [7].

doi: 10.1109/EUROSOI-ULIS49407.2020.9365285 - ©2021 IEEE. Personal use is permitted, but republication/redistribution requires IEEE permission.

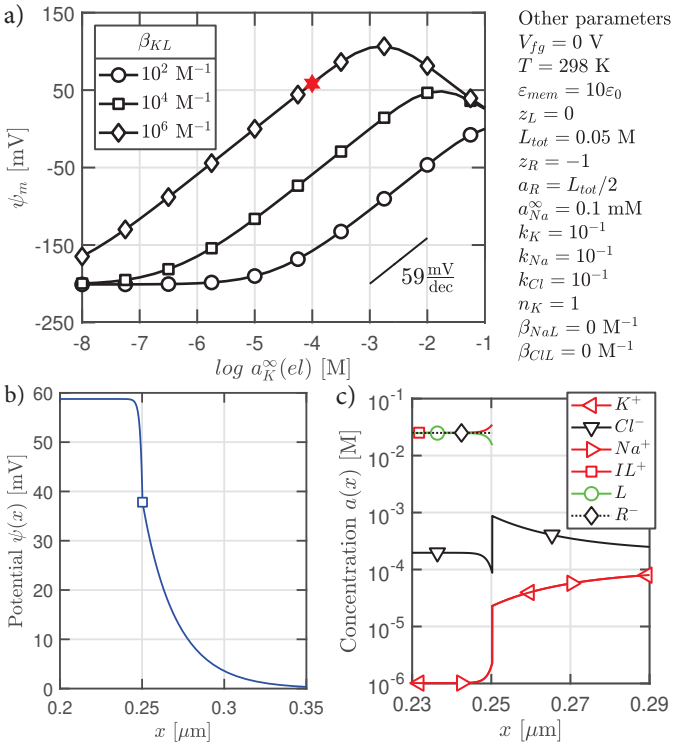

Fig. 5. a) Effect of ionophore-target ion (KL^+) association constant β_{KL} on membrane potential for different K^+ concentrations in the electrolyte. Here, only one reaction is considered (i.e. complexes such as ClL or NaL are neglected for simplicity). b) and c) are the potential and concentration spatial distributions for $a_K = 0.1$ mM and $\beta_{KL} = 10^6$ M^{-1} (red mark in a)). In c) red, black and green line colors refer to positive, negative and neutral ion valences. The thicknesses of the membrane and electrolyte are 250 nm and 2 μm respectively. Bulk concentrations specified in the figure refer to the electrolyte layer.

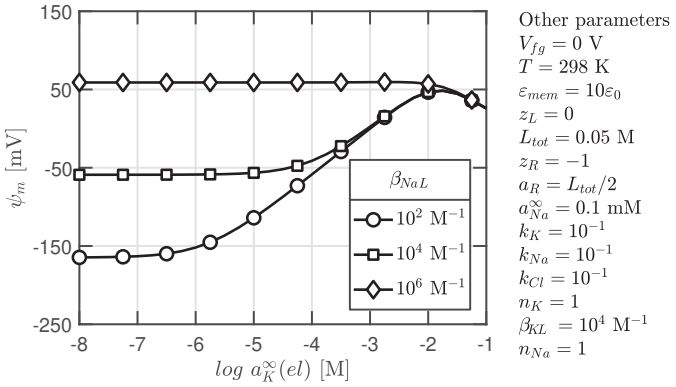

Fig. 6. Impact of ionophore-interferent ion (NaL^+) association constant β_{NaL} on membrane potential for different target ion K^+ concentrations in the electrolyte. Here, the formation of two complexes (KL and NaL with 1:1 stoichiometries) are considered.

When target co-ions react with ionophores, cross-sensitivity issues arise. These are due to the reduced capacity of the membrane to fix the concentration of target ions inside. Such phenomenon is related to both the binding constants strength of the IL and JL complexes, and the concentration of interferent species. An example is provided in Fig. 6. Here, the membrane response with respect to the target ion K^+ is simulated for different binding constants of the ionophore-interferent ion complex, NaL^+, for constant concentration of the interferent ion. For simplicity, we used equal affinity values for all ions and considered only 1:1 stoichiometries. As expected, we observe that the lower limit of detection is directly proportional to the binding constant β_{NaL}. For β_{NaL}=β_{KL}=10^4, there is no membrane preference between target and interferent ions, giving that a membrane response only appears when $a_K^{\infty} > a_{Na}^{\infty}$, while stronger ionophore-interferent than ionophore-target complexes (β_{NaL}=10^6) eventually lead to no membrane response.

V. Conclusions

We developed a 1D model coupling distributed chemical reactions between ionic species and ionophores in ISMs and the PB equation for equilibrium. We showed the fundamental role of ionic sites in determining the sensor response. When including ionophores, we further investigated the impact of binding constants on the membrane performance, showing that the full response can be shifted towards lower concentrations for improved sensitivity. The (currently 1D) model is amenable to 3D implementation and to further extensions of the set of electrochemical processes. The insights gained on ISM operation with FET devices aim to support improvements in sensor performances and assist the search for new sensor applications.

References

[1] S. D. Moss, J. Janata, and C. C. Johnson, "Potassium ion-sensitive field effect transistor," *Analytical Chemistry*, vol. 47, no. 13, pp. 2238–2243, 1975. DOI: 10.1021/ac60363a005

[2] A. Cao, M. Mescher, D. Bosma, J. H. Klootwijk, E. J. R. Sudhölter, and L. C. d. Smet, "Ionophore-Containing Siloprene Membranes: Direct Comparison between Conventional Ion-Selective Electrodes and Silicon Nanowire-Based Field-Effect Transistors," *Analytical Chemistry*, vol. 87, no. 2, pp. 1173–1179, 2015. DOI: 10.1021/ac504500s

[3] P. Bergveld, "A critical evaluation of direct electrical protein detection methods," *Biosensors and Bioelectronics*, vol. 6, no. 1, pp. 55–72, 1991. DOI: 10.1016/0956-5663(91)85009-l

[4] E. Bakker, E. Pretsch, and P. Bühlmann, "Selectivity of Potentiometric Ion Sensors," *Analytical Chemistry*, vol. 72, no. 6, pp. 1127–1133, 2000. DOI: 10.1021/ac991146n

[5] S. Amemiya, P. Bühlmann, and K. Odashima, "A Generalized Model for Apparently Non-Nernstian Equilibrium Responses of Ionophore-Based Ion-Selective Electrodes. 1. Independent Complexation of the Ionophore with Primary and Secondary Ions," *Analytical Chemistry*, vol. 75, no. 14, pp. 3329–3339, 2003. DOI: 10.1021/ac026471g

[6] P. Bühlmann, L. Yahya, and R. Enderes, "Ion-Selective Electrodes for Thiocyanate Based on the Dinuclear Zinc(II) Complex of a Bis-N,O-bidentate Schiff Base," *Electroanalysis*, vol. 16, no. 12, pp. 973–978, 2004. DOI: 10.1002/elan.200302937

[7] E. Bakker, "Ion-selective electrodes — overview," in *Encyclopedia of Analytical Science (Third Edition)*, P. Worsfold, C. Poole, A. Townshend, and M. Miró, Eds. Oxford: Academic Press, 2019, pp. 231 – 251. ISBN 978-0-08-101984-9. [Online]. Available: http://www.sciencedirect.com/science/article/pii/B9780124095472143641

[8] H. Girault, "Charge Transfer across Liquid-Liquid Interfaces," in *Modern Aspects of Electrochemistry*. Springer, 1993, pp. 1–62. ISBN 978-1-4613-6247-0

[9] R. P. Buck and E. Lindner, "Recommendations for nomenclature of ionselective electrodes (IUPAC Recommendations 1994)," *Pure and Applied Chemistry*, vol. 66, no. 12, pp. 2527–2536, 1994. DOI: 10.1351/pac199466122527